Propagation of Subpicosecond Laser Pulses through a Fully Ionized Plasma

P. E. Young and P. R. Bolton

Lawrence Livermore National Laboratory, University of California, P.O. Box 5508, Livermore, California 94550

(Received 20 May 1996)

Propagation of subpicosecond laser pulses through a fully ionized plasma has been studied experimentally. Measurements of the light transmitted through the plasma and of the light scattered at 90 deg to the beam show the onset and growth of relativistic filamentation. Frequency-resolved optical gating of the transmitted pulse shows motion of electrons into and out of the beam. [S0031-9007(96)01708-5]

PACS numbers: 52.35.Fp, 52.35.Mw, 52.40.Nk, 52.50.Jm

The development of high intensity lasers has led to the possibility of observing relativistic effects when a laser pulse interacts with a fully ionized plasma. The propagation of high intensity laser pulses through a fully ionized plasma is a basic physics problem of great interest which also has practical applications for compact x-ray lasers [1,2], laser-plasma-based particle accelerators [3], and advanced inertial confinement fusion schemes [4]. The relativistic filamentation instability can lead to modifications of the propagating pulse by spatially modulating the laser intensity transverse to the direction of propagation. The relativistic filamentation and self-focusing instabilities, [5], have been studied theoretically for a number of years, and are important because one needs to understand the laser propagation at high intensities before one can interpret the results from other nonlinear phenomena [6,7]. Previous experimental studies of high-intensity laser pulses have employed neutral gases which are ionized by the propagating pulse [8]. That technique is limited by technical constraints to relatively low electron densities ($\leq 10^{19}$ cm^{-3}) and introduces the possibility of the modification of the propagation behavior by the formation of an ionization front at the leading edge of the pulse [8].

In this Letter, we describe an experiment in which a high intensity (up to 5×10^{18} W/cm^2), 600 fsec laser pulse propagates through a fully ionized preformed plasma of substantial density (up to $0.5n_c$, where n_c is the critical density at which the laser frequency, ω_0, equals the plasma frequency, ω_p). When the laser intensity, I_L, and plasma density, n_e, are sufficiently low such that relativistic filamentation does not grow, the pulse channels through the plasma. As I_L or n_e is increased, we observe the onset of relativistic filamentation, in which the beam breaks up into multiple hot spots, as opposed to whole-beam self-focusing, by analyzing the light transmitted through the plasma and by 2D pictures of the sidescattered laser light. If the plasma density or the laser intensity is high enough, the beam breakup occurs before the pulse reaches the peak plasma density. Along with the beam breakup, we observe time-dependent spectral modulation of the laser pulse transmitted through the plasma using a frequency-resolved optical gating (FROG) diagnostic. In the early part of the pulse we observe a spectral redshift, consistent with electrons being moved out of the beam path, followed by a spectral blueshift, signaling the collapse of the channel.

The experiment was performed using the Janus laser facility at Lawrence Livermore National Laboratory. One beam of the laser produced a 0.53 μm wavelength, 45 J, 1.3 ns long, nominally square laser pulse that irradiated a 0.5 μm thick polypropylene exploding foil target (CH_2) which is supported by a 75 μm thick Mylar washer. This beam is focused with an $f/4$ lens to a 400 μm diameter spot. After the plasma forming pulse has burned through the target and the peak density has decayed below n_c, a second, interaction pulse counterpropagates relative to the plasma forming beam through the plasma. This pulse has a central wavelength of 1.053 μm with a bandwidth of 1.4 nm, and is compressed to a FWHM pulse width of $\sim$600 fs with a contrast ratio of 10^{-5} as measured by a third order autocorrelation technique. The pulse is compressed and propagated to the target entirely in vacuum. The 6.5 cm diameter beam is focused by a 30 cm focal length off-axis parabola to a focused spot with a FWHM diameter of 12 μm (confocal parameter of 260 μm) which was measured with an equivalent plane imaging system. At the highest input energies (6 J) the maximum intensity at best focus is $\sim 5 \times 10^{18}$ W/cm^2. The energy was varied during the course of the experiment by rotating a polarizer in the amplifier chain to eject some of linearly polarized laser light before it reaches the vacuum compressor.

Light that is transmitted through the plasma is collected by the focusing lens of the plasma forming lens. A dielectric mirror for 1.053 μm directs the transmitted picosecond light to a dielectric beam splitter; 50% of the light goes to an energy calorimeter and 50% goes to a single-shot FROG diagnostic [9]. The calorimeter therefore records the amount of the light collected by the lens. For the case where the focused beam is undeflected (no plasma), all of the incident energy is collected by the lens. The FROG diagnostic records the laser spectrum versus time with 10 fs resolution. We have used the polarization gated version of FROG in which optical gating occurs within a thin fused silica Kerr slide [9].

The target plasma density distribution was measured by a folded wave interferometer throughout the experiment. The probe beam for the interferometer was 0.35 μm

 0031-9007/96/77(22)/4556(4)$10.00

wavelength, 600 fs in duration, and was timed to within 50 ps of the arrival of the interaction pulse at the target. In appropriate cases we are able to observe the density channel formed by the subpicosecond pulse.

We also imaged the sidescattered 1.053 μm light transverse to the propagation direction of the ps pulse in order to locate the position of the maximum laser intensity. The scattered light is imaged with an $f/4$ camera lens which forms a magnified image at a CCD camera with a resolution of about 10 μm. The lens views the laser light at an angle of 45 deg with respect to the direction of incident polarization. The camera is filtered with a bandpass filter to observe only light within ± 50 Å of the incident laser wavelength. Regardless of the production process for this scattered light, our observation of density perturbations with similar spatial structure (discussed below) observed in the scattered light pictures leads us to believe that the pictures represent the regions where the laser pulse is most intense.

The onset of relativistic filamentation is shown quite clearly in the scaling of the collected transmitted energy with the incident beam energy (see Fig. 1). As we found in earlier, 100 ps experiments [10], filamentation can result in the spraying out of the transmitted light to angles much larger than the vacuum propagation angle. In Fig. 1, we see that at low laser intensities, the transmitted laser energy equals the incident energy, which is consistent with inverse bremsstrahlung lengths from 3 mm ($n_e = 0.2n_c$, $T_e = 1$ keV) to 1.5 cm ($n_e = 0.05n_c$, $T_e = 0.5$ keV). Above an intensity of 10^{18} W/cm^2, the percentage of transmitted light is less as the filamentation instability increases. Varying the peak density changes the laser intensity at which the inflection point occurs. For a peak density of $0.1n_c$, the transition occurs near 0.15 J, while for a peak density of $0.05n_c$, it occurs near 0.7 J. The maximum amount of light backscattered into the parabola was 10% and cannot account for the transmission behavior.

The power at which the transition occurs in Fig. 1 is greater than the predicted critical power for relativistic self-focusing:

$$P_c = 17(n_c/n_e)\ \mathrm{GW}. \quad (1)$$

Substituting the measured peak densities into this equation gives critical powers of $P_c = 340$ GW or $E_c = 200$ mJ for $n_e = 0.05n_c$, and $P_c = 170$ GW or $E_c = 100$ mJ for $n_e = 0.1n_c$. The threshold energies are higher than those given by the theory probably because the theory is linear, whereas in the actual experiment the high-intensity pulse can depress the background density. The paraxial approximation used in the theory will also predict a lower threshold than if finite *f*-number focusing is used as in the experiment [11].

We verified the deflection of the transmitted light using high-speed infrared film filtered with 2 mm thick RG1000 to record the light outside the collecting lens. The experiment showed that as the energy was increased, the light sprayed to larger angles (up to 50° from the laser axis for $I = 2 \times 10^{18}$ W/cm^2, and $n_e = 0.3n_c$), consistent with the observed decrease in the transmitted energy [10]. We filtered portions of the film with a high reflector for 1.053 μm light and with a 1 cm thick KDP crystal, which absorbs stimulated Raman scattered (SRS) light with wavelengths longer than 1.4 μm, to show that most of the sprayed light has wavelengths close to the fundamental laser wavelength and the contributions from SRS are small. This result is consistent with the simulations of Ref. [12] which predict a 20% reduction of transmitted light due to SRS absorption and scattering. It has also been pointed out [13] that SRS will not occur in evacuated channels. Previous experiments [14] in which a single pulse interacts with a gas jet have observed large amounts of SRS at densities ($0.01n_c$) which are five times lower than our lowest density. As the gas fill pressure (electron density) increased, the forward SRS anti-Stokes feature decreased to the detection noise level, accompanied by the exponential increase of the transmitted laser light; this was attributed to self-focusing and ionization induced refraction (which cannot occur in our experiment), results which are consistent with those of our experiments.

We believe that Eq. (1) is the proper prediction to compare to our experiment rather than ponderomotive filamentation based on the argument that the ions do not have time during the laser pulse to move out of the beam. That time is given by [5,15]: $\Delta t_i \sim 140 r_\mu (I_{18}\lambda_\mu^2)^{-1/4}$ fs, where r_μ is the radius of the laser beam in microns, I_{18} is the laser intensity in 10^{18} W/cm^2, and λ_μ is the laser wavelength in microns. For $r_\mu = 6$, and $I_{18} = 1$, $\Delta t_i \sim$ 800 fs, which is longer than the laser pulse length.

The image of the sidescattered laser light shows a systematic behavior as the peak density is varied (see Fig. 2). We observe a horizontal region of emission that is due to scattering of the laser light from the plasma and a vertical image of the target illuminated by rescattered laser light. At the lowest density, the image shows that the light remains focused through the peak of the plasma to the far side. Increasing the peak density reduces the extent of this

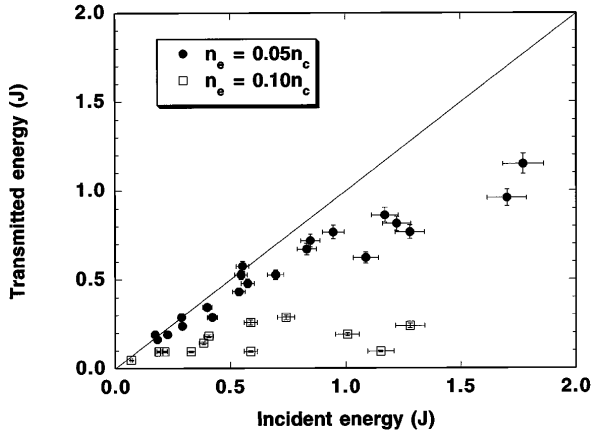

FIG. 1. Measured energy transmitted through the plasma as a function of the incident energy for two different peak plasma densities.

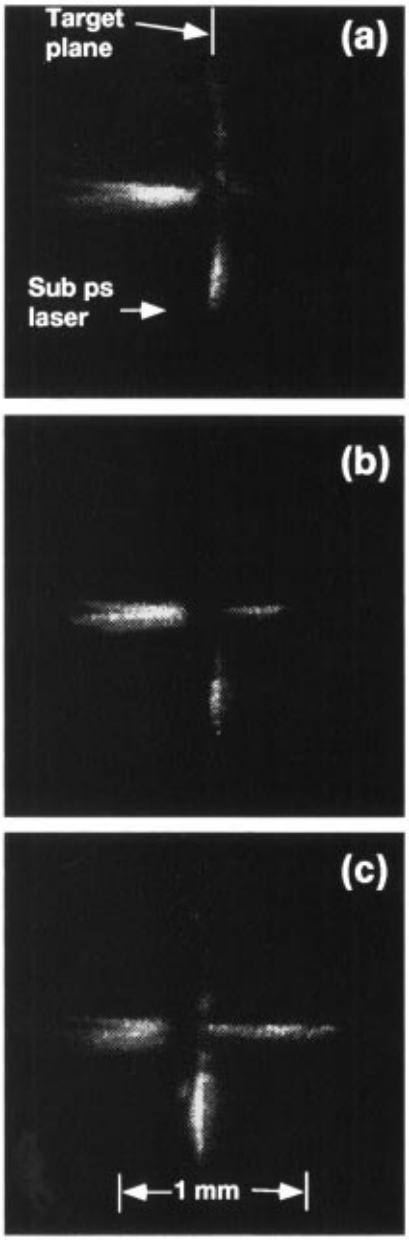

FIG. 2. Sidescattered transmitted light pictures for peak densities of (a) 0.35, (b) 0.20, and (c) $0.05n_c$ with an incident laser energy of 500 mJ.

focused region until, at the highest density, the emission region is limited to the incident side of the plasma, and is significantly brighter. This is consistent with increased spraying of the light via filamentation as one exceeds the instability threshold.

A sample interferogram is shown in Fig. 3; each fringe in this picture represents a 2π phase shift of the probe with respect to the reference beam due to the electron density. We see the density channel on the right hand side of the target in the interferograms, as well as density structure on the input side of the target in the vicinity of the bright emission region seen in the side images. The length of the channel seen in the interferogram agrees with

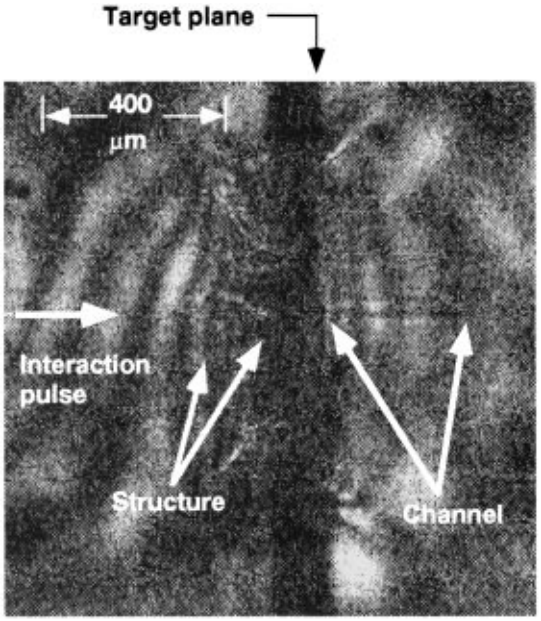

FIG. 3. Interferogram for a case where the peak density is $0.20n_c$ and the incident laser energy is 500 mJ.

that seen in the scattered light pictures as the peak density is varied, as well; both pictures show channels that are 35 μm in diameter. These results show that the scattered light pictures [compare to Fig. 2(b)] are related to where the laser intensity is the highest.

Time and spectrum resolved measurements of the light transmitted through the plasma further elucidate the channel formation process. Since the path to the FROG diagnostic is through a window and 5 m of air, *B*-integral effects due to the nonlinear index of refraction can lead to a slight spectral chirp and lengthen the *measured* pulse as seen in Fig. 4(a) for an incident energy of 500 mJ. The vertical axis is the calibrated FROG time which should be divided by a factor of ~ 3 to recover the actual pulse time in the vacuum chamber. This intensity dependent effect is proven by comparison with a lower intensity vacuum pulse (<10 mJ) which gives a signal that matches the autocorrelation measurement; this is not a problem as long as we compare signals of comparable energy with and without a plasma.

Figure 4(b) shows one of the analyzed signals for a peak density of $0.2n_c$ and 500 mJ incident energy, showing the transmitted energy and spectral shifts as a function of time. Part of the apparent shortening of the pulse is probably due to the spraying of the light which can reduce the amount of light reaching the FROG during the first half of the pulse; this can be seen to occur prior to $t = 0$. For comparison, some pulse compression can result from group velocity dispersion due to the difference between the propagation times of the pulse through the evacuated channel and through the higher density walls. Using the relativistic index of refraction, N, [5], we find that the pulse lengthening is given by $\Delta\tau = (N - 1)l_z/c$, where l_z

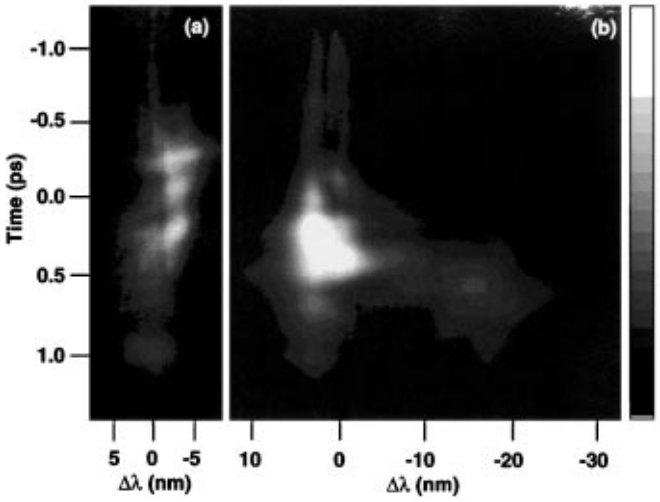

FIG. 4. Recorded FROG signal (a) without a plasma, and (b) for the conditions of Fig. 2(b). The gray scale is linear and ranges from 0 (black) to 5×10^5 (white) counts.

is the length of the channel, which we choose to be the size of the emission region on the left hand side of the channel seen in Fig. 2. For an average background density of $0.25 n_c$, we find that $N = 0.9$, so at most $\Delta\tau = 100$ fs even if $l_z = 300$ μm, so we conclude that this does not have a substantial effect.

During the first half of the pulse [see Fig. 4(b)], we observe a redshift of $\sim$30 Å, which is expected if the electrons are being pushed out of the beam. Light propagating through a plasma with a time-dependent electron density undergoes a frequency shift given by [16]: $\Delta\omega(t) = -\frac{\partial}{\partial t}\int_{x_1}^{x_2} k\, dx$, where x_1 and x_2 represent the spatial limits of the plasma and k is the wave number of the light in the plasma. One can rewrite this as

$$\frac{\Delta\lambda}{\lambda} = \frac{1}{2}\,\frac{L}{c}\,\frac{d(n/n_c)}{dt}, \qquad (2)$$

where L is the path length through the plasma. Taking $d(n/n_c) = 0.20$, $dt = 0.5$ psec, then $L = 5$ μm in order to match $\Delta\lambda/\lambda = 2.8 \times 10^{-3}$ as we observe in the experiment. This assumes full evacuation of the filament; we expect the maximum wavelength shifts to occur in the regions of highest intensity. The calculated L is consistent with the filament lengths observed in models [10].

The late time FROG signal [see Fig. 4(b)] shows a blueshifted feature with a wavelength shift of about 150 Å which occurs on a more rapid time scale than the redshift in the early part of the pulse. Using $d(n/n_c) = 0.20$, $dt = 0.1$ psec, and $L = 5$ μm in Eq. (2) gives $\Delta\lambda = 150$ Å. At higher peak densities ($>0.3 n_c$) the blueshifted feature is modulated at a period of 100 fs; this frequency equals the plasma frequency at a density of 1×10^{18} cm^{-3} which might be the density inside the filaments. One possible interpretation of the FROG trace is that there is a relatively slow formation of density cavities followed by a rapid collapse of the filaments similar to the caviton collapse that has been discussed in the literature (see, for example, Ref. [17]). Laser-produced caviton formation has recently been studied both theoretically [13,18] and experimentally [19].

In summary, we have experimentally investigated laser light propagation through a preformed underdense plasma. We observe beam breakup above a threshold intensity consistent with relativistic filamentation. Unlike prepared index cases, this is not a whole-beam effect; therefore the transmission is reduced greatly in the channeling regime.

We acknowledge useful discussions with M. Feit, J. Garrison, and A. Rubenchek. We also thank J. Bonlie, W. Cowens, J. Foy, A. Hankla, J. Hunter, G. London, and B. Sellick for technical assistance. This work was performed under the auspices of the U.S. Department of Energy by the Lawrence Livermore National Laboratory under Contract No. W-7405-Eng-48.

[1] C. E. Clayton *et al.*, Phys. Rev. Lett. **70**, 37 (1993).
[2] P. Sprangle and E. Esarey, Phys. Fluids B **4**, 2241 (1992), and references therein.
[3] N. H. Burnett and P. B. Corkum, J. Opt. Soc. Am. **6**, 1195 (1989); D. C. Eder *et al.*, Phys. Plasmas **1**, 1744 (1994).
[4] M. Tabak *et al.*, Phys. Plasmas **1**, 1626 (1994).
[5] C. E. Max *et al.*, Phys. Rev. Lett. **33**, 209 (1974); G. Z. Sun *et al.*, Phys. Fluids **30**, 526 (1987); P. Sprangle *et al.*, Trans. Plasma Sci. **PS-15**, 145 (1987); W. B. Mori *et al.*, Phys. Rev. Lett. **60**, 1298 (1988); X. L. Chen and R. N. Sudan, Phys. Rev. Lett. **70**, 2082 (1993); E. Esarey *et al.*, Phys. Rev. Lett. **72**, 2887 (1994); P. Gibbon *et al.*, Phys. Plasmas **2**, 1305 (1995).
[6] P. Sprangle and E. Esarey, Phys. Rev. Lett. **67**, 2021 (1991).
[7] P. Monot *et al.*, Phys. Rev. Lett. **74**, 2953 (1995).
[8] R. Rankin *et al.*, Opt. Lett. **16**, 835 (1991); P. Monot *et al.*, J. Opt. Soc. Am. B **9**, 1579 (1992); A. J. Mackinnon *et al.*, Phys. Rev. Lett. **76**, 1473 (1996); P. R. Bolton *et al.*, J. Opt. Soc. Am. B **13**, 336 (1996).
[9] R. Trebino and D. J. Kane, J. Opt. Soc. Am. A **10**, 1101 (1993); D. J. Kane and R. Trebino, Opt. Lett. **18**, 823 (1993); D. J. Kane and R. Trebino, IEEE J. Quantum Electron. **29**, 571 (1993).
[10] S. C. Wilks *et al.*, Phys. Rev. Lett. **73**, 2994 (1994); P. E. Young *et al.*, Phys. Plasmas **2**, 2825 (1995).
[11] P. R. Bolton and B. E. Ritchie, J. Opt. Soc. Am. (to be published).
[12] K.-C. Tzeng *et al.*, Phys. Rev. Lett. **76**, 3332 (1996).
[13] P. Mora and T. M. Antonsen, Jr., Phys. Rev. E **53**, R2068 (1996).
[14] C. A. Coverdale *et al.*, Phys. Rev. Lett. **74**, 4659 (1995).
[15] W. B. Mori and T. Katsouleas, Phys. Rev. Lett. **69**, 3495 (1992).
[16] E. Yablonovitch, Phys. Rev. Lett. **31**, 877 (1973).
[17] D. DuBois *et al.*, Phys. Scr. **T30**, 137 (1990), and references therein.
[18] A. Pukhov and J. Meyer-ter-Vehn, Phys. Rev. Lett. **76**, 3975 (1996).
[19] D. Umstadter *et al.*, Science **273**, 472 (1996).